

Development of Lorentz-force-type Slotless Active Magnetic Bearing

Satoshi Ueno and Shin-ichi Uematsu

*Department of Mechanical Engineering
Faculty of Science and Technology
Ritsumeikan University
1-1-1 Nojihigashi, Kusatsu, Shiga 525-8577, Japan
sueno@se.ritsumei.ac.jp*

Takayuki Arai and Kinya Odagiri

*Namiki Precision Jewel Co., Ltd.
5-1, Aza Koyashikizoe Oaza Shimomenaisawa
Kuroishi-City Aomori 036-0539, Japan*

Abstract—Magnetic bearings have advantages such as no friction loss, no abrasion, lubrication free operation, and so on. However they are not used widely due to their high cost and large size. In order to solve these problems, an active magnetic bearing having a simple structure with distributed windings is proposed. The rotor consists of a permanent magnet and an iron yoke, which rotate in a body. The stator consists of a 3-phase distributed winding and is installed between a permanent magnet and a back yoke of the rotor. A Lorentz-force is generated by the stator current, and the rotor position is controlled by this force. In this paper, the bearing force is analyzed theoretically, and its control method is shown. A simple experiment confirmed that the proposed AMB can be realized.

Index Terms – Active magnetic bearing, digital control, Lorentz force, rotary machinery

I. INTRODUCTION

In recent years, the demand for improving the durability of small motors and reducing the noise generated by them has been increasing [1,2,3]. A magnetic bearing is advantageous in solving these problems. Various types of small motors that use an active magnetic bearing (AMB) or a self-bearing motor has been proposed. However, the AMB is not in widespread use since it is expensive and its dimensions are very large as compared with those of mechanical bearings. As a result, the development of a smaller and relatively low cost AMB is desired.

In order to meet this demand, a 6-salient-pole-type AMB has been proposed. This AMB has achieved miniaturization and low cost by reducing the number of salient poles and coils in the conventional magnetic bearing. However, since the miniaturization and large bearing force are reconciled, the structure has become complicated. As a result, further miniaturization of the 6-salient-pole-type AMB is difficult, and a simpler structure is required.

In recent years, the miniaturized brushless DC motor has been developed. In particular, the miniaturization of a slotless stator type motor has been remarkable and it is commercially available as a motor 2 mm in diameter. Since the magnetic bearing has a structure that is similar to

the brushless motor, it can form a small magnetic bearing by utilizing the structure of a micro brushless DC motor.

In this paper, a Lorentz-type AMB with a simpler structure is proposed. A distribution winding without a core is installed in a stator, and a cylindrical permanent magnet fixed to a back yoke is attached to a rotor. Here, the pole number of the stator winding is set as plus or minus 2 pole of the rotor permanent magnet - the similar to that of a self bearing motor. A radial force is then generated by the Lorentz-force produced by the stator current and the magnetic field produced by the permanent magnet. Usually, the force that can be generated by an AMB employing the Lorentz-force is small in comparison with that generated by a typical magnetic bearing [4]. Due to this reason, it is necessary to supply a large current in order to nullify the unstable force of the permanent magnet. However, this results in a decrease in the efficiency. In order to resolve this problem, the permanent magnet of the rotor is fixed to the yoke; consequently, the unstable force of the permanent magnet becomes zero. The proposed magnetic bearing has a simple structure. Therefore, both miniaturization and low cost can be realized.

In this paper, the relation between the current and bearing force is derived from the relation between the positions of the winding and the permanent magnet. Moreover, it is shown that it is possible to control the bearing force. The result obtained from the analysis is then confirmed using a simple experimental setup.

II. SLOTLESS AMB

The outline of the proposed AMB is shown in Figure 1 and 2. The AMB performs position control with two radial degrees of freedom. A cylindrical 2-pole permanent magnet and a yoke are attached to the rotor. The unstable force of the permanent magnet then becomes zero. The stator consists of a 3-phase 4-pole distributed winding without a core, and it is inserted between the permanent magnet and the yoke of the rotor.

The principle of force generation is shown in Figure 2. For simplification, the figure illustrates the case in which the number of turns of the stator winding is 1. If a 3-phase current is fed through the stator winding, a Lorentz-force is generated as shown in the figure. Since the winding is fixed to the stator, a radial force is generated on the rotor as a reaction force. The radial force is controlled by

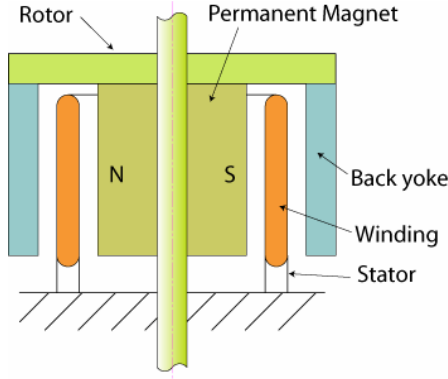


Fig. 1 Schematic of Slotless AMB

changing of the amplitude and the phase of the 3-phase current.

A. Radial Force

The radial direction forces have been derived. A coordinate system is defined as shown in Figure 2. The turn portion of the winding end is not taken into consideration; it is assumed that each wire is arranged along the axial direction of the rotor. Then the distribution of the 3-phase 4-pole winding of n turns is expressed as follows:

$$\begin{aligned}
 \theta_{+u}^k &= \theta_0 + \frac{k-1}{3n}\pi, \theta_0 + \frac{k-1}{3n}\pi + \pi \\
 \theta_{+v}^k &= \theta_0 + \frac{k-1}{3n}\pi + \frac{2}{6}\pi, \theta_0 + \frac{k-1}{3n}\pi + \frac{8}{6}\pi \\
 \theta_{+w}^k &= \theta_0 + \frac{k-1}{3n}\pi + \frac{4}{6}\pi, \theta_0 + \frac{k-1}{3n}\pi + \frac{10}{6}\pi \\
 \theta_{-u}^k &= \theta_0 + \frac{k-1}{3n}\pi + \frac{3}{6}\pi, \theta_0 + \frac{k-1}{3n}\pi + \frac{9}{6}\pi \\
 \theta_{-v}^k &= \theta_0 + \frac{k-1}{3n}\pi + \frac{5}{6}\pi, \theta_0 + \frac{k-1}{3n}\pi + \frac{11}{6}\pi \\
 \theta_{-w}^k &= \theta_0 + \frac{k-1}{3n}\pi + \frac{7}{6}\pi, \theta_0 + \frac{k-1}{3n}\pi + \frac{1}{6}\pi
 \end{aligned} \quad (1)$$

where θ is the angular position of the wire, the subscript of θ denotes the phase of the current and its direction, k is the number of the winding, and θ_0 is the angular position of the first +u phase wire. The direction that goes to surface from the back of the sheet is defined as positive.

In order to simplify the analysis, it is assumed that the magnetic field generated by the current is small as compared to that generated by the permanent magnet of the rotor, and the sine wave distribution of the magnetic flux density is obtained. Then, the distribution of the magnetic flux density is expressed as

$$B_g = B \cos(\theta - \varphi) \quad (2)$$

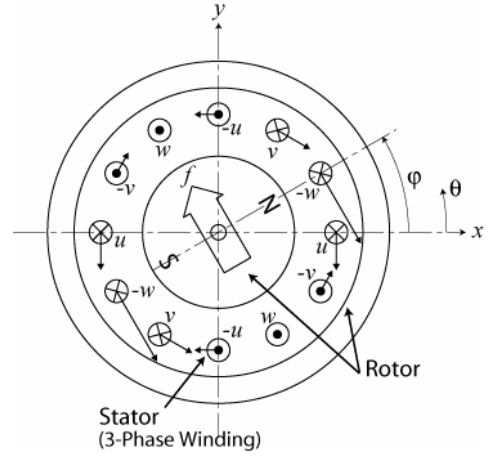


Fig. 2 Principle of Giving Bearing Force

where B is the amplitude of magnetic flux density, and φ is the rotational angle of the rotor. The 3-phase through each phase of the stator is defined as follows.

$$\begin{aligned}
 i_u &= A \cos(\phi) \\
 i_v &= A \cos(\phi - 2\pi/3) \\
 i_w &= A \cos(\phi - 4\pi/3)
 \end{aligned} \quad (3)$$

where A is the amplitude of the current, and ϕ is the phase of the stator current.

The direction of the Lorentz-force on the wire is tangential and its magnitude is

$$\begin{aligned}
 f_r|_{+phase}^k &= B_g(\theta_{+phase}^k) \cdot l \cdot i_{+phase} \\
 f_r|_{-phase}^k &= -B_g(\theta_{-phase}^k) \cdot l \cdot i_{-phase}
 \end{aligned} \quad (4)$$

where l is the axial length of the wire. The x and y direction forces generated by the wire become

$$\begin{aligned}
 f_x|_{\pm phase}^k &= -f_r|_{\pm phase}^k \sin(\theta_{\pm phase}^k) \\
 f_y|_{\pm phase}^k &= f_r|_{\pm phase}^k \cos(\theta_{\pm phase}^k)
 \end{aligned} \quad (5)$$

The total force is the summation of (5), and radial direction force of the rotor is the reaction force of the stator winding. Then, we have

$$f_x = -\sum_{k=1}^n f_x|_{\pm phase}^k \quad (6)$$

$$f_y = -\sum_{k=1}^n f_y|_{\pm phase}^k$$

For $n = 1$, equation (6) becomes

$$\begin{aligned}
 f_x &= -3ABl \sin(\varphi - \phi + 2\theta_0) \\
 f_y &= -3ABl \cos(\varphi - \phi + 2\theta_0)
 \end{aligned} \quad (7)$$

For $n = 3$, the interval between wires phases is $\pi/9$. Therefore, the radial force becomes the summation of (7) where substituted by $\theta_0 = -\pi/9, 0, \pi/9$. Then, we have

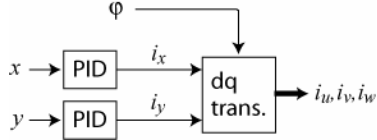


Fig. 3 Block Diagram of Controller

$$\begin{aligned} f_x &= -3ABl \sin(\phi - \varphi) \{1 + 2 \cos(2\pi/9)\} \\ f_y &= -3ABl \cos(\phi - \varphi) \{1 + 2 \cos(2\pi/9)\} \end{aligned} \quad (8)$$

Similarly, the following equations will be obtained.

$$\begin{aligned} f_x &= -3cBlA \sin(\phi - \varphi) \\ f_y &= -3cBlA \cos(\phi - \varphi) \end{aligned} \quad (9)$$

where

$$\begin{aligned} c &= 1 + 2 \cos\left(\frac{2\pi}{3n}\right) + 2 \cos\left(\frac{4\pi}{3n}\right) + \dots \\ &\quad + 2 \cos\left(\frac{(n-1)\pi}{3n}\right) \end{aligned}$$

This result shows that the radial forces are controlled by A and $\phi - \varphi$.

Next, the stator current is expressed using d-q transform

$$\begin{bmatrix} i_u \\ i_v \\ i_w \end{bmatrix} = \begin{bmatrix} \cos \varphi & \sin \varphi \\ \cos(\varphi - 2\pi/3) & \cos(\varphi - 2\pi/3) \\ \cos(\varphi - 4\pi/3) & \cos(\varphi - 4\pi/3) \end{bmatrix} \begin{bmatrix} i_y \\ i_x \end{bmatrix} \quad (10)$$

Then the radial forces become

$$\begin{aligned} f_x &= 3cBli_x \\ f_y &= -3cBli_y \end{aligned} \quad (11)$$

Hence the radial forces can be controlled by i_x and i_y .

B. Modeling and Controller

The dynamic equation is derived. The rotor magnet and the back yoke are fixed; then, the permanent magnet does not generate an unbalance force. Thus, neglecting the gyro effect, the dynamic equation becomes

$$\begin{bmatrix} \dot{x} \\ \ddot{x} \\ \dot{y} \\ \ddot{y} \end{bmatrix} = \begin{bmatrix} 0 & 1 & 0 & 0 \\ 0 & 0 & 0 & 0 \\ 0 & 0 & 0 & 1 \\ 0 & 0 & 0 & 0 \end{bmatrix} \begin{bmatrix} x \\ \dot{x} \\ y \\ \dot{y} \end{bmatrix} + \frac{3kBl}{m} \begin{bmatrix} 0 & 0 \\ 1 & 0 \\ 0 & 0 \\ 0 & -1 \end{bmatrix} \begin{bmatrix} i_x \\ i_y \end{bmatrix} \quad (12)$$

In this paper, a PID controller is used for stabilizing (12). A block diagram of the controller is shown in Figure 3.

III. EXPERIMENTAL RESULT

A. Experimental Setup

In order to validate the above results, a simple experimental setup was designed and tested. The experimental setup is shown in Figure 4. For

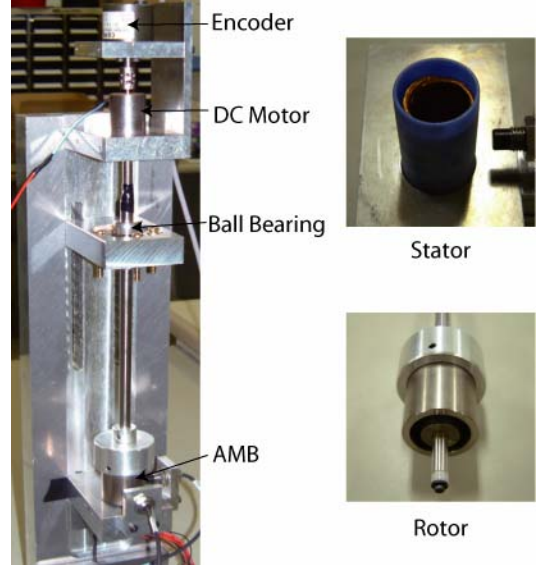


Fig. 4 Experimental Setup

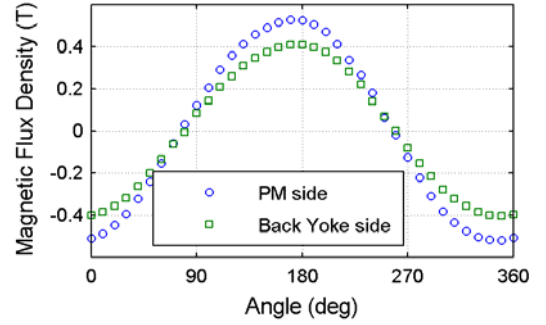


Fig. 5 Magnetic Flux Density Distribution

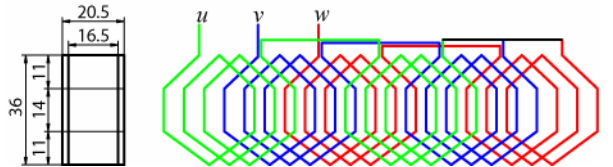


Fig. 6 Stator Winding

simplification, the rotor top was supported with a ball bearing; therefore, the rotor has two degrees of freedom. The AMB was attached to the lower part of the rotor, while a DC motor and a rotary encoder were attached to the upper part of the rotor, for providing rotation and measuring rotor angular position, respectively.

The rotor consists of a shaft, a permanent magnet, a back yoke, and one part to fix them together. A Sm-Co 2-pole permanent magnet was used. The diameter of the permanent magnet is $\phi 15.2$ mm, and its length is 32 mm. The back yoke is made of S45C. The outer diameter of the back yoke is $\phi 30$ mm and its inner diameter is $\phi 23.5$ mm. The magnetic flux density distribution between the permanent magnet and the back yoke is shown in Figure 5.

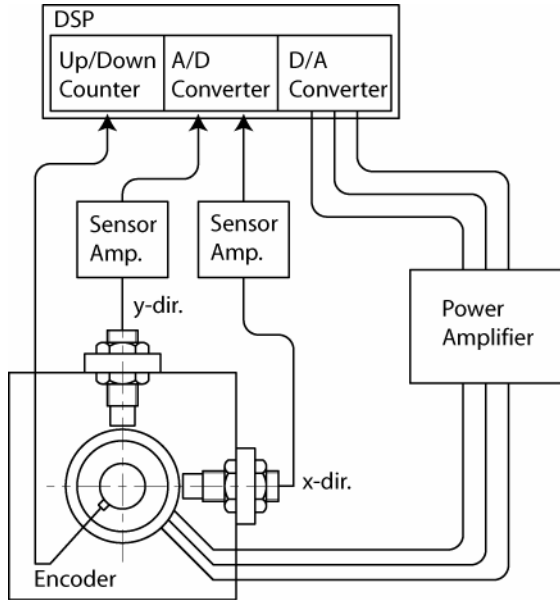


Fig. 7 Control System

The circle denotes the results of PM side measurement and the square denotes the results of back yoke side. From these results, it is confirmed that the magnetic flux density distribution is sinusoidal, and its average amplitude is about 0.42 T.

The stator consists of the winding and a plastic collar for fixing it. The 3-phase 4-pole distributed winding is used as shown in Figure 6. The electric wire is coiled as shown in the drawing on the right-hand side of Figure 6 and then it is wound cylindrically. Therefore the central part of the winding is in parallel to the axial direction, while the upper and lower parts are slanted to turn them downward. The copper wire used has a diameter of $\phi 0.18\text{mm}$ and the number of turns is 103. Variable c in (9) becomes 85.2.

The control system is shown in Figure 7. A DSP has been used for control. The DSP receives the signals from two displacement sensors through AD converters and calculates the control currents to each axis using a PID controller. The control currents are then converted into stator currents based on the rotation angle information obtained using an encoder. The stator currents are then outputted to power amplifiers through DA converters. Then, the power amplifier feeds the current as a command value by current feedback.

B. Radial Force

The measurement results of the bearing force are shown in Figure 8. While performing position control of the rotor, a constant disturbance force was applied in the x direction, and the current was measured when the displacement became zero. The horizontal axis represents the bearing force, and the vertical axis represents the control current. The circles and squares denote the i_x and i_y values,

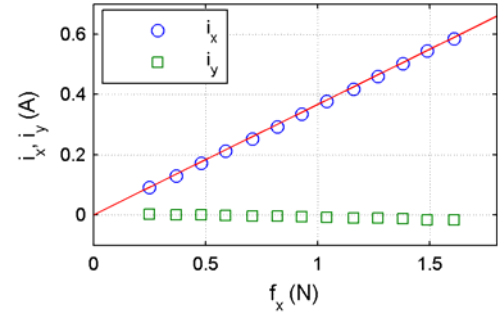


Fig. 8 Radial Force

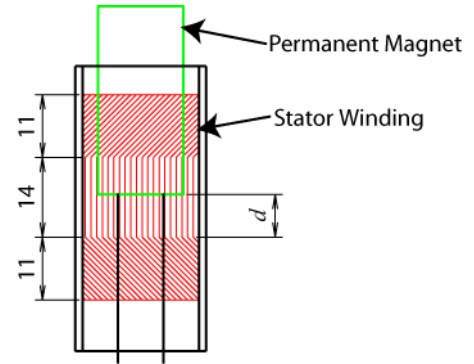


Fig. 9 Position of Rotor and Stator

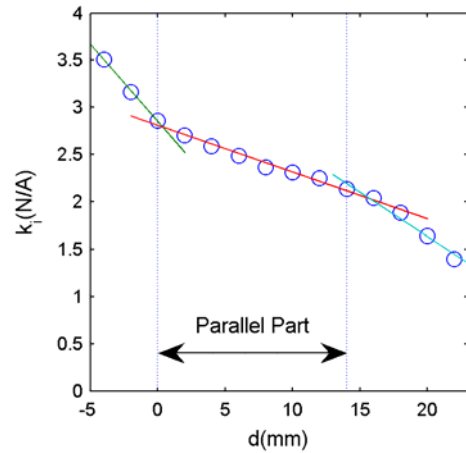
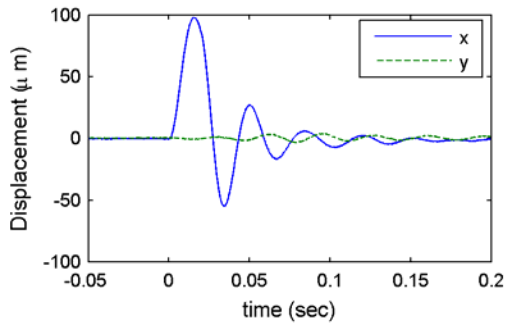


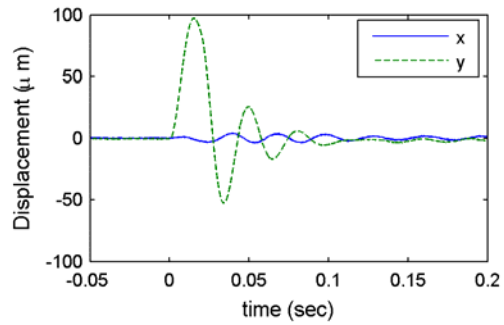
Fig. 10 Gain Characteristics

respectively. This result shows that the force is proportional to the current.

Next, the positions of the permanent magnet of the rotor and the stator winding were changed and the radial force was measured. The relative positions of the rotor and the stator are shown in figure 9. The force factor of the radial force for the current when changing d in Figure 9 was measured. The result is shown in Figure 10. The force factor decreases as d increases. This rate becomes 49.5 N/(Am) on the parallel portion. The theoretical value is 107 N/(Am) from (11). The experimental result was approximately half of the theoretical value. It is considered that one reason for this is that the experimental device was not ideal.



(a) x-axis



(b) y-axis

Fig. 11 Impulse Responses

C. Impulse Response

The impulse response was measured to confirm the position control performance. The results are shown in Figure 11. Figure 11 (a) shows the response on the x-axis when the disturbance is along the x-direction and (b) shows response in the y-direction. Both impulse responses settled in 0.1 s, and confirmed that stable control was performed.

C. Rotation Test

Next, the rotation test was performed. The orbits of the rotor at 590 rev/min and 2062 rev/min are shown in Figure 12. Both have a distorted form. This is considered to be caused by the influence of the unbalance of the rotor, run out of the sensor, and the manufacture error of the stator winding.

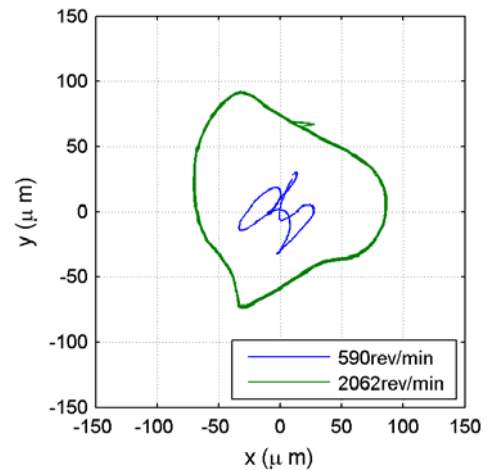


Fig. 12 Orbit of Rotor

IV. SUMMARY

In this paper, a slotless AMB that employs a distribution winding with a simple structure was proposed. Through analysis and experiment, it was shown that the proposed AMB can be realized.

In the future, the relation between the winding and the bearing force will be investigated in greater detail, and the motor will be made to function as a self-bearing motor by the addition of a motor winding.

REFERENCES

- [1] Y. Okada et al., JSME Publication on New Technology Series, No. 1, Magnetic Bearings—Fundamental Design and Applications, Yokendo Ltd. Tokyo, 1995, in Japanese (translated into Korean).
- [2] S. Ueno et al., “Development of the Miniature AMB with 6 Concentrated Wound Poles”, ISMB-9, Lexington, KY, USA, 2004
- [3] L. Li et al., “A Simple and Miniaturized Magnetic Bearing for Cost-Sensitive Applications”, Proc of 8th Int. Symp. on Magnetic Bearings, Mito, August 26–28, 2002, pp. 561–565.
- [4] T. Tokumoto et al., “Comparison between Slot and Slotless Constructions of Lorenz Type Self-bearing Motor”, Trans. of JSME, Vol. 68, No. 674 C, pp. 2992–2998, 2002, in Japanese